A&A 381, L53–L56 (2002)
DOI: 10.1051/0004-6361:20011652

Astronomy & Astrophysics

Knot production in magnetized Herbig–Haro jets

M. Thiele and M. Camenzind

Landessternwarte Königstuhl, 69117 Heidelberg, Germany

Received 23 April 2001 / Accepted 22 November 2001

Abstract. We present the results of a simulation of an axisymmetric (2.5–dimensional), magnetized Herbig–Haro jet. The parameters are chosen for a typical collimated outflow from a young stellar low–mass object. We show that the nose–cone feature of 2D MHD jets critically depends on the magnetic field topology of the precollimation mechanism. The most prominent features of our model jet are knot–like structures along the jet axis which develop in the foremost part of the jet. Shocks associated with these internal knot–like structures mimic bow–shock like features as seen in Herbig–Haro flows.

Key words. stars: HH objects – magnetohydrodynamics: jets and outflows – cooling: forbidden emission lines

1. Introduction

Herbig–Haro (HH) jets are ejected from the very youngest stars, which are mostly still deeply embedded into their parental clouds (Reipurth 1997). The essential parameters of HH jets are well determined by observations (Hartigan et al. 1994; Ray et al. 1997; Reipurth et al. 1997; Eislöffel & Mundt 1998; Bacciotti & Eislöffel 1999). Two contrasting views about the nature of HH jets have been proposed: (i) the jet beams could be susceptible to Kelvin–Helmholtz (KH) instabilities and observations of knots have been interpreted in the light of this model (Bührke et al. 1988; Eislöffel & Mundt 1992); (ii) others saw jets as highly transient and variability in the jet source would lead to internal working surfaces traveling along the jet axis (Stone & Norman 1993; Reipurth et al. 1997).

It is generally accepted, that HH jets are highly supersonic (with sonic Mach number $M = 10 \ldots 40$), overdense plasma flows (density contrast $\eta = \rho_{\rm j}/\rho_{\rm ex} = 1 \ldots 10$), which take their origin in the ultimate vicinity of young low–mass stars and propagate through their hosting molecular cloud, finally terminating in a double shock structure (HH objects). However, the cause for the most prominent morphological features of HH jets, the emission line knots and their usually non–straight shape (wiggling) is still not clear. Due to the complexity of the involved interactions, numerical simulations are practically the only means to study the mechanisms at work. The wiggling as a real 3D feature cannot be studied by simulations of axisymmetric jets. Emission line knots can however also be observed in unusually straight jets as HH 34 (Bührke et al. 1988) and HH 212 (Zinnecker et al. 1998). Thus, it should be possible to study the knot production mechanisms also by simulations of axisymmetric jets. Only those potential knot production mechanisms which work in the axisymmetric case are reliable candidates also for the corresponding 3D case, since an imposed axisymmetry rather promotes both the production and the survival of such morphological features as knots. Knot production mechanisms that only work in the 3D case can hardly account for knots in straight jets as HH34 and in addition obviously require low Mach numbers in the pure hydrodynamic case (Xu et al. 2000). Time–dependent ejection of matter at the jet base and fluid instabilities are the most frequent explanations for knot production. For this purpose, numerical simulations with time–dependent boundary conditions at the inlet were performed (Raga et al. 1990; Stone & Norman 1993; Suttner et al. 1997; Stone & Hardee 2000; O'Sullivan & Ray 2000). Time–dependent ejection certainly occurs on long time scales leading to multiple HH objects (Reipurth et al. 1997; Zinnecker et al. 1998). But the emission line knots themselves are at least not generally due to episodic ejection, since there are knots without any indication of an internal working surface (Ray et al. 1996). In addition, it seems that episodic ejection cannot account for the low values of the ratio between the knot velocity and the velocity of the gas (Eislöffel et al. 1998). The possibility of generating knots by KH–instabilities (de Gouveia Dal Pino & Birkinshaw 1996; Micono et al. 1998), MHD Kelvin–Helmholtz instabilities (Cerqueira & de Gouveia Dal Pino 1999) and by current–driven modes (Frank et al. 2000) was extensively studied.

In this letter, we present the results of a simulation for an axisymmetric, magnetized jet. In the first section we give a detailed description of the underlying model and in Sect. 2 we present and discuss our results.

Send offprint requests to: M. Thiele,
e-mail: mthiele@lsw.uni-heidelberg.de

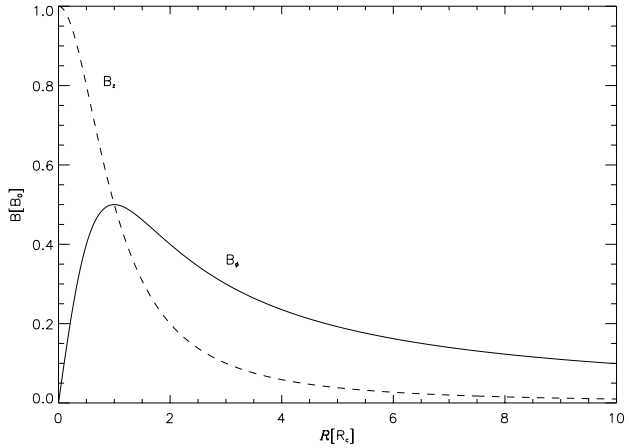

Fig. 1. Profiles of the poloidal (dashed line) and the toroidal (solid line) magnetic field component at the inlet; only the toroidal part was used in this simulation.

2. Magnetic structure of Herbig–Haro jets

Herbig–Haro jets are modelled within the framework of ideal MHD, by implementing numerically the 3D–MHD code NIRVANA (Ziegler 1995). A homogeneous and five times overdense cylindrical beam with a radius of $R_\mathrm{j} \approx 100\,\mathrm{AU}$ propagates through an initially uniform, stationary, ambient medium. The numerical grid has an extension of $\Delta R \times \Delta z = 1.5 \times 10^{16} \times 2.25 \times 10^{17}\,\mathrm{cm}^2$. This corresponds to 10 jet radii in the radial and 150 jet radii in the axial direction. The area is resolved by $N_R \times N_z = 150 \times 2250$ grid cells. Thus 15 cells span the jet radius. The propagation of the jet was followed, until it had reached the upper z–boundary, corresponding to observed jet lengths.

Initial and boundary conditions: Along the axis of symmetry ($R = 0$) reflecting boundary conditions and on all other sides of the computational domain outflow boundary conditions were used. Only on a circular region around the symmetry axis at the lower z–boundary ($z = 0, R \le R_\mathrm{j}$), the boundary conditions correspond to inflow of a super-magnetosonic cylindrical beam, which carries a toroidal magnetic field, given by the analytic solution of the transverse force–equilibrium (Camenzind 1997)

$$B_\phi = -\frac{R}{R_\mathrm{c}} \frac{B_0}{1+(R/R_\mathrm{c})^2}, \quad z=0,\, R \le R_\mathrm{j}, \tag{1}$$

$$B_z = \frac{B_0}{1+(R/R_\mathrm{c})^2}, \quad z=0,\, R \le R_\mathrm{j}. \tag{2}$$

The expression contains the core radius R_c as a characteristic length scale. For $R < R_\mathrm{c}$, the toroidal magnetic field increases linearly with radius, beyond R_c it decreases as $1/R$ (Fig. 1). In the absence of a poloidal field, the radial force equilibrium requires a corresponding radial profile for the thermal pressure

$$p = p^{(0)} - \frac{B_0^2}{8\pi}\left[1 - \frac{1}{(1+R^2/R_\mathrm{c}^2)^2}\right], \; z=0,\, R \le R_\mathrm{j}, \tag{3}$$

$$p^{(0)} = p_\mathrm{a} + \int_0^{R_\mathrm{j}} \frac{B_\phi(R')^2}{4\pi R'}\,\mathrm{d}R'. \tag{4}$$

The inclusion of a poloidal field component on the boundary poses a technical problem, since it demands that it has to be extended to the integration domain as an initial condition. Otherwise $\nabla\cdot\boldsymbol{B} = 0$ would not be fulfilled. This is the reason why most 2D jet models either only involve toroidal fields or a poloidal field that does not depend on z initially. It results in an ambient medium which is considerably magnetized right from the beginning. This can only be avoided if a bent field structure is found that matches the profiles on the boundary of the grid. Reasonable initial configurations should therefore guarantee the following constraints (Thiele 2000): (i) $\nabla\cdot\boldsymbol{B} = 0$ globally; (ii) decreasing magnetic energy density both in the axial and in the radial direction; (iii) if possible, analytical expressions. We have found analytical solutions to this mathematical problem for both the 2D and the 3D case (Thiele 2000; Thiele & Camenzind, in prep.). A numerical solution of this problem was found by Kössl et al. (1990).

The jet velocity depends on the radius,

$$v_z = v^{(0)} \cos\left((4\pi/9)\, R/R_\mathrm{j}\right), \quad z=0,\, R \le R_\mathrm{j}, \tag{5}$$

and guarantees an approximately constant magnetosonic Mach number on the jet cross section. For the velocity of the jet on the symmetry axis we have chosen $v^{(0)} = 100\,\mathrm{km\ s^{-1}}$. On the boundary the jet has no radial and no toroidal velocity component, thus $v_R = v_\phi = 0$, $z = 0, R \le R_\mathrm{j}$. The ambient medium is initially homogeneous, stationary and unmagnetized. Both $p^{(0)}$ and p_a denote the central jet pressure and the ambient pressure for the case of an equilibrium between jet and ambient medium at their interface. Since we intended to establish an initially overpressured jet we have taken a modified value for the ambient pressure ($p = \alpha\, p_\mathrm{a}$). The jet is essentially characterized by 4 parameters: the density ratio $\eta = \rho_\mathrm{j}/\rho_\mathrm{a} = 5$, the magnetosonic Mach number $M_\mathrm{ms} = v_\mathrm{j}/c_\mathrm{ms} = 6$ (c_ms = magnetosonic velocity), the plasma–beta $\beta := p_\mathrm{th}/p_\mathrm{mag} = 0.35$ and α ($\approx$6.5). The values of these parameters are averages over the jet cross section. Note that the low value of the magnetosonic Mach number is not chosen arbitrarily but is motivated by the theory of jets for the associated stationary case which gives values $M_\mathrm{ms} = 2\ldots3$ (Fendt & Camenzind 1996; Lery & Frank 2000). Usually, molecular clouds are highly inhomogeneous and even turbulent (Zinnecker et al. 1998). Thus, both density and pressure vary in space and time. Often superposed is a large scale variation of both decreasing and increasing density/pressure with increasing distance from the central young star (Fuller & Myers 1992). Thus, jets are expected to experience phases of expansion and recollimation (Eislöffel & Mundt 1994). The former "stochastic" density/pressure distribution can only be incorporated into models of real 3D jets (Thiele 2000; Thiele & Camenzind, in prep.), whereas the large–scale density/pressure distribution can also be incorporated in models of 2D jets.

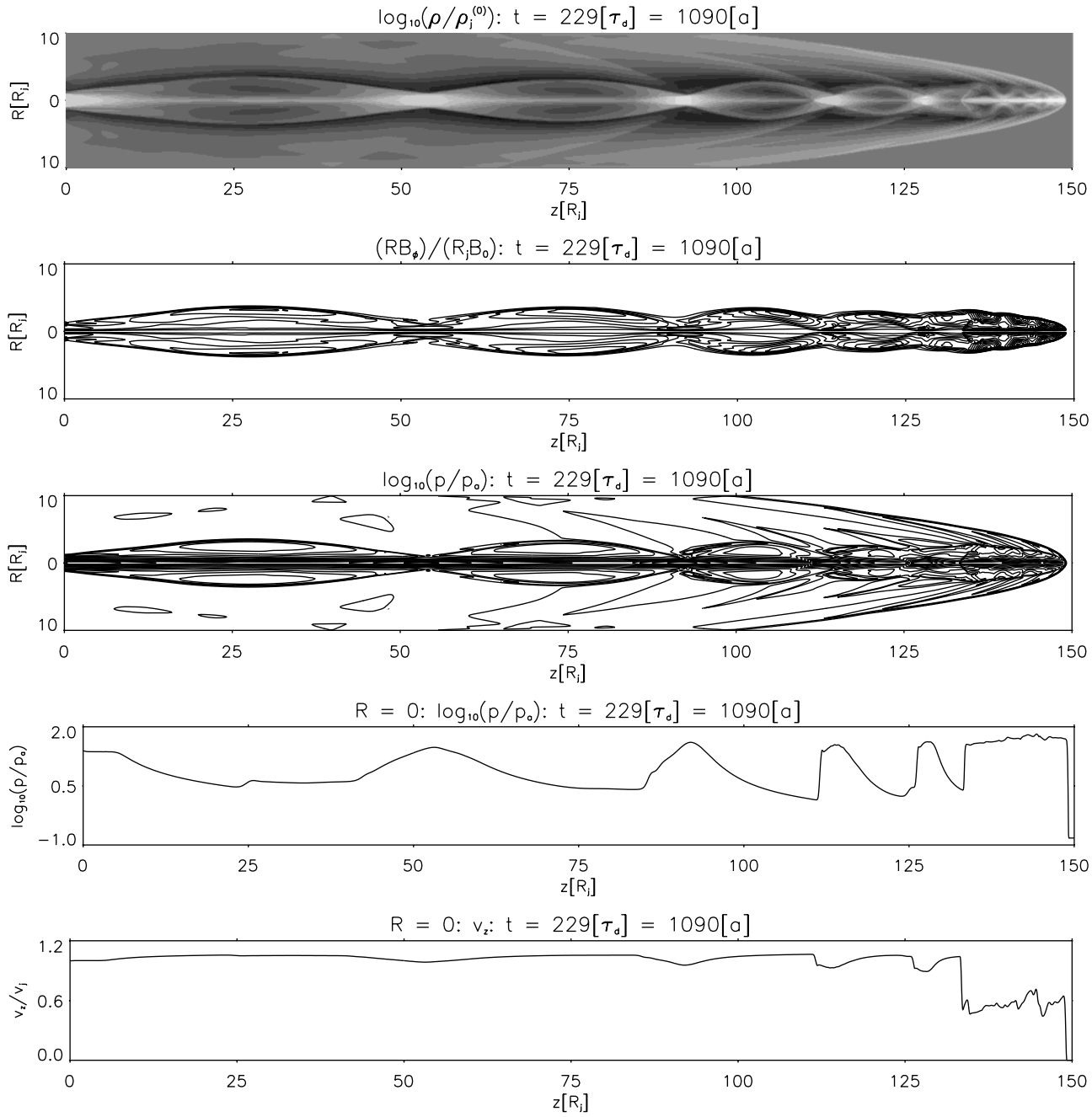

Fig. 2. From up to down: grey-scale image of the density, iso–contour lines of the current and the pressure, axial profiles of the pressure and the z–component of the jet velocity on the jet axis; the Mach disk is located at $z \approx 134$.

3. Knots propagating in Herbig–Haro jets

The jet radius R_j is the fundamental length scale, time is normalized to dynamical time–scale, $\tau_\mathrm{d} := R_\mathrm{j}/v_\mathrm{j}$, and velocities are expressed in units of $v^{(0)}$. For comparison with observations three quantities are of major importance: the ratio between the pattern speed (knot velocity) and the gas velocity, $\zeta := v_\mathrm{k}/v_\mathrm{g}$ (Eislöffel & Mundt 1992), the ratio between the knot spacing and the jet diameter, $\delta := d_\mathrm{k}/D$ (Bührke et al. 1988), and the distance between the bow shock (bs) and the Mach disk (ms), $\xi := z_\mathrm{bs} - z_\mathrm{ms}$.

Since the jet is initially overpressured, it widens right from the beginning. This is followed by a recollimation towards the axis, which is due to the action of both the external pressure and of the toroidal magnetic field (Fig. 1). The recollimation results in the typical X–like shock pattern on the axis, where the shock is reflected. The cycle is repeated several times along the jet axis. By far more interesting are structures which develop near the jet head due to the initial perturbations. This can be seen in the density scale plot of Fig. 2 which shows a snapshot of the jet at its final state at $t = 229$. For this structure, the magnetic field profile is of decisive importance. The idea that the knot pattern seen in HH jets might be an alternating expansion and recollimation due to an initially

overpressured hydrodynamic jet was proposed quite early in the history of jet modelling (Falle et al. 1987). But these pure hydrodynamic models predict stationary knot patterns, in contrast to observations; the knots move with velocities somewhat smaller than the jet velocity (Eislöffel & Mundt 1992, 1994, 1998). In addition, the ratio between the inter–knot distance and the jet diameter comes out to be at least $\delta \geq 10$, whereas the observed values are in the range $\delta = 1 \ldots 3$ (Bührke et al. 1988). In early alternative models, the knots were attributed to the action of the first order reflection mode of the Kelvin–Helmholtz instability, which results indeed in a non–stationary knot pattern (Payne & Cohn 1985). But the high Mach numbers ($M \geq 40$) and density ratios $\eta = 1 \ldots 10$, derived for several protostellar jets, lead to rather high values for the knot spacing, $\delta \lesssim 10$. The inclusion of magnetic fields can cure the most important of these shortcomings. But in this context the profile of the magnetic field inside of the jet is decisive and should be motivated by the theory. The ratio $R_\mathrm{c}/R_\mathrm{j}$ deeply influences the development of some major morphological features, such as the nose–cone. For $R_\mathrm{c}/R_\mathrm{j} \ll 1$, the magnetic field inside the jet has effectively a core–envelope structure. If the toroidal field component ($\beta \leq 1$) achieves its maximum near the jet surface, $R_\mathrm{c}/R_\mathrm{j} \lesssim 1$, a huge nose–cone develops (Clarke et al. 1986; Lind et al. 1989; Frank et al. 2000). On the other hand, the nose–cone can be avoided very easily, if the toroidal field does not culminate in the outer zones but well inside the jet (Stone & Hardee 2000). For the final state of our simulation we derive $z_\mathrm{ms} \approx 134$ and $\xi \approx 15$. Since $R_\mathrm{c} = 0.2 \ll R_\mathrm{j}$, the axial extension of the nose–cone is significantly reduced. A further reduction of the core radius R_c would result in the disappearence of this structure. Thus, the question whether nose–cones can be avoided in simulations of 3D jets is just of minor importance, they already can be suppressed in the 2D case.

Knot–like structures only appear for magnetosonic Mach numbers of the order of a few. This indicates that these structures are determined by the magnetic field and the magnetosonic Mach number. The resulting pattern moves with a velocity somewhat smaller than the jet velocity. For the foremost knots we derive $\zeta \approx 0.55$, which is in accordance with the observed values ($\zeta = 0.5 \ldots 1$). For the ratio between the knot spacing and the jet diameter we obtain $\delta \approx 1{-}1.5$. Observed values lie in the range $\delta \approx 1{-}4$ (HH 34: $\delta \approx 3$; Bührke et al. 1988). In our simulation this small knot spacing is essentially caused by a correspondingly low value of the magnetosonic Mach number which is motivated by theoretical arguments (Sect. 2). It is to be expected that a slightly larger value would result by taking an emission property. Furthermore the extension of the foremost knots is larger in the transverse than in the longitudinal direction, which seems to agree with observations (Zinnecker et al. 1998). We do not claim that only these foremost 3 knots correspond to the knots that are observed in protostellar jets. But they are continously produced in the jet head and move backward along the jet beam resulting in a chain of knots. This becomes obvious by regarding time sequences. As shown by the behaviour of the pressure along the jet axis (Fig. 2), shock structures are associated with each of these internal knots. These features, which are reminiscent of inner bow shocks, are driven into the already shocked jet and ambient gas. In our simulation, these structures are found to be less prominent in the pressure countours than in the density, due to high pressure in the cocoon (neglecting cooling).

2D MHD models for Herbig–Haro flows already reveal the main observed characteristics of dynamics and morphology. The inclusion of cooling and of a poloidal field component can change somewhat the above results. Furthermore it has to be checked wether the mechanism also works in the 3D case. The simulation presented here is only one out of a series of simulations for different parameter ranges. A more detailed study for the 3D case will follow.

Acknowledgements. MT's research has been supported by the Deutsche Forschungsgemeinschaft (DFG) through the Schwerpunktprogramm *Physik der Sternentstehung*.

References

Bacciotti, F., & Eislöffel, J. 1999, A&A, 342, 717
Blondin, J. M., Fryxell, B. A., & Königl, A. 1990, ApJ, 360, 370
Bührke, T., Mundt, R., & Ray, T. 1988, A&A, 200, 99
Camenzind, M. 1997, IAU Symp., 189, 241
Cerqueira, A. H., & de Gouveia Dal Pino, E. M. 1999, ApJ, 510, 828
Clarke, D. A., Norman, M. L., & Burns, J. O. 1986, ApJ, 311, L63
de Gouveia Dal Pino, E. M., & Birkinshaw, M. 1996, ApJ, 471, 832
Eislöffel, J., & Mundt, R. 1992, A&A, 263, 292
Eislöffel, J., & Mundt, R. 1994, A&A, 284, 530
Eislöffel, J., & Mundt, R. 1998, AJ, 115, 1554
Falle, S. A. E. G., Innes, D. E., & Wilson, M. J. 1987, MNRAS, 225, 741
Fendt, C., & Camenzind, M. 1996, A&A, 313, 591
Frank, A., Lery, T., et al. 2000, ApJ, 540, 342
Fuller, G. A., & Myers, P. C. 1992, ApJ, 384, 523
Hartigan, P., Morse, J. A., & Raymond, J. 1994, ApJ, 436, 125
Kössl, D., Müller, E., & Hillebrandt, W. 1990, A&A, 229, 378
Lery, T., & Frank, A. 2000, ApJ, 533, 897
Lind, K. R., Payne, D. G., et al. 1989, ApJ, 344, 89
Micono, M., Massaglia, S., et al. 1998, A&A, 333, 1001
O'Sullivan, S., & Ray, T. P. 2000, A&A, 363, 3550
Payne, D. G., & Cohn, H. 1985, AJ, 291, 655
Raga, A. C., Binette, L., Canto, J., & Calvet, N. 1990, ApJ, 364, 601
Ray, T. P., Mundt, R., et al. 1996, ApJ, 468, L103
Ray, T. P., Muxlow, T. W. B. et al. 1997, Nature, 385, 415
Reipurth, B. 1997, in IAU Symp., 189, 3
Reipurth, B., Bally, J., & Devine, D. 1997, AJ, 114, 2708
Stone, J. M., & Norman, M. L. 1993, ApJ, 413, 198
Stone, J. M., & Hardee, P. E. 2000, ApJ, 540, 192
Suttner, G., Smith, M. D., et al. 1997, A&A, 318, 595
Thiele, M. 2000, Dissertation, Universität Heidelberg
Xu, J., Hardee, P. E., & Stone, J. M. 2000, ApJ, 543, 161
Ziegler, U. 1995, Dissertation, Universität Würzburg
Zinnecker, H., McCaughrean, M. J., & Rayner, J. T. 1998, Nature, 394, 862